Case Studies in Thermal Engineering 36 (2022) 102092

Contents lists available at ScienceDirect

Case Studies in Thermal Engineering

journal homepage: www.elsevier.com/locate/csite

Experimental comparison of heat transfer characteristics of Enhanced Truck Radiators

Hatice Mercan [a,*], Furkan Sonmez [b], Ahmet Selim Dalkilic [c], Somchai Wongwises [d,e]

[a] Department of Mechatronics Engineering, Yildiz Technical University, Yildiz, Besiktas, 34349, Istanbul, Turkey
[b] Ford Trucks, Sancaktepe R&D Center, Sancaktepe, 34885, Istanbul, Turkey
[c] Department of Mechanical Engineering, Yildiz Technical University, Yildiz, Besiktas, 34349, Istanbul, Turkey
[d] Department of Mechanical Engineering, King Mongkut's University of Technology Thonburi, Bangkok, 10140, Thailand
[e] National Science and Technology Development Agency (NSTDA), Pathum Thani, 12120, Thailand

A R T I C L E I N F O

Keywords:
Heat exchanger
Enhanced tubes
Antifreeze
Heat transfer rate
Pressure drop
ε-NTU Method

A B S T R A C T

In the current experimental investigation, the radiators' heat transfer performances are evaluated experimentally and validation is done using the analytical ε-NTU method. In this experimental study composition of the cooling fluid is 50:50 water/EG. The pressure and temperature values are fixed for air and water/ethylene glycol sides. The velocity of air is between 1.5 – 12 m/s and water/ethylene glycol flow rate is between 2.5 – 7 kg/s. All measurements are performed after steady state is reached. For altering operation conditions, the overall heat transfer coefficient, exit water/ethylene glycol temperature, pressure drop and friction coefficients are evaluated experimentally. Both rate of heat transfer and the pressure drop are maximum for the double U grooved case. For the tested radiator categories, the overall heat transfer coefficient rose with increasing coolant and air velocity and the exit temperature raised with increased coolant flow rate and decreased with increasing velocity of air.

1. Introduction

Thermal performance and the radiator design are two major components that shape the overall efficiency of the heavy trucks. For unvarying inlet temperature and pressure, the performance of four dissimilar heavy truck radiators is considered with altering water/ethylene glycol flow rate and air velocity. The essential variables for the optimal thermal performance are disclosed using the design parameters and the operating conditions. In the literature review, all range of vehicle radiators are included because there are few studies focusing on heavy trucks and they are summarized in the following paragraph.

Charyulu et al. [1] investigated the impact of dissimilar materials in the fin and tube production of diesel engine radiators and reported similar HT and PD characteristics for brass, copper and carbon steel. Rahmatinejad et al. [2] investigated the optimum engine radiator size for identical operating conditions. The experimental results are validated with a genetic algorithm. The optimum number of fins is reported as 436 with a size of 2.867 mm, where the size, cost and weight of the heat exchanger reduced significantly. Akpobi et al. [3] performed and FEM analysis to evaluate the velocity and temperature variation in the radiator tubes. They reported the necessity of dense meshing in the vicinity of the inlets and exits to have more accurate solutions. In the experimental investigation Hamid et al. [4] studied the HT performance of hybrid nanofluid in a circular tube with wire coil inserts. The results are presented for 0.5–3.0% volumetric concentration of TiO_2–SiO_2 hybrid nanofluids, Re number 2300–12000 and pitch ratio of 0.83–4.17. The

* Corresponding author.
E-mail address: hmercan@yildiz.edu.tr (H. Mercan).

https://doi.org/10.1016/j.csite.2022.102092
Received 2 March 2022; Received in revised form 30 April 2022; Accepted 2 May 2022
Available online 21 May 2022
2214-157X/© 2022 The Authors. Published by Elsevier Ltd. This is an open access article under the CC BY-NC-ND license (http://creativecommons.org/licenses/by-nc-nd/4.0/).

optimum performance is reported for 1.5 pitch ratio and 2.5% concentration. Bilen et al. [5] investigated the grooved tube friction and HT characteristics for turbulent flow regime. Three different groove geometries are compare and trapezoidal grooves performed superior up to Re = 30000 and rectangular grooves performed better up to Re = 28000 compared to circular tubes. The optimum entropy generation is reported at Re = 17000 for all groove geometries. Murugesan et al. [6] investigated the HT and PD in square cut twisted and plane twisted tube inserts under turbulent flow regime for altering twist ratios and 2000<Re<12000. The square cut tape inserts showed significantly higher performance in HT however the PD also increased significantly compared to plain cut tape inserts. They also introduced Nusselt number and friction coefficient equations for square and plane twisted tapes. Eiamsa-Ard et al. [7] studied the rib grooved tube flow and reported the turbulent heat transfer characteristics under uniform heat flux. The comparison was performed for altering configurations of the triangular rib, triangular groove and rectangular rib. Rectangular rib and triangular groove performed significantly better compared to other combinations hydro-thermally. The effect of pitch ratio also studied to introduce equations for Nusselt number, friction coefficient and enhancement index. The heat transfer and friction characteristic of R-134a in a corrugated pipe heat exchanger is investigated experimentally (Loahalertdecha et al. [8]). They conducted the experiments for constant hot water Re number, Re = 5500, and a range of cold stream Re number 3500<Re<18000. For altering convex and concave corrugated tube configurations the maximum performance is reported for concave corrugated outer and convex corrugated inner pipe version. Ji et al. [9] performed a comparison study with corrugated tube and plane tube heat exchangers fro altering pitch heights and mass fluxes for R-134-a. They reported a better hydro-thermal performance of corrugated pipe compared to plain version. In a literature summary Mohammed et al. [10] performed a comparison study for different pipe geometries for hydro-thermal performance and concluded that the internally finned tubes performed significantly better than other tube configurations and for dimpled and corrugated pipes the PD rise is insignificant compared to their superior thermal enhancement. Finally, especially at turbulent regime the twisted tape inserts reported to perform with a low efficiency however they might be preferable for high viscous flows and low to moderate Re number regimes. The symmetry and zigzag shaped trapezoidal corrugated tubes are investigated by Ajeel et al. [11] numerically. Four nanofluids (Al_2O_3, CuO, SiO_2, and ZnO) are compared for a range of concentration, 1–4%, and 500<Re<20000 and aspect ratio of groove with 0.5–4. Trapezoidal grooves performed better thermally and SiO_2 resulted with highest Nusselt number. The best performing base fluid is reported as glycerin. In an experimental study Kcheril and Elias [12] investigated the radiator performance for automobile engines and compared aluminum based nanofluids and nanosized ferro fluids. They observed a better heat transfer performance with ferrofluids compared to aluminum nanofluids. To reduce the radiator size and weight and improve the efficiency Salamon et al. [13] investigated the TiO_2 nano fluid experimentally. They reported a better performance of traditional EG/water mixture at low inlet coolant temperature however at higher operating temperatures the TiO_2 nano fluid improved the HT rate with 8.5% compared to EG/water mixture. Goudarzi and [14] conducted an experimental study to study the influence of Al_2O_3-EG nanofluid and wire coil inserts in vehicle heat exchangers. The experiments are conducted for two dissimilar wire cross sections and three increasing concentration of nanofluids. The synchronized use of wire inserts and nanofluids performed 5% better than the case with only wire inserts used. The high performance vehicle engines require higher energy removal. In the experimental study Said et al. [15] investigated the radiators with Al_2O_3 /EG:DW and TiO_2 /EG:DW. They performed a comparison based on the thermophysical characteristics and stability at long term of the two nanofluids. They observed 24.21% thermal performance improvement with the Al_2O_3 /EG:DW. Shahsavani et al. [16] proposed a compact correlation function of temperature and particle concentration using available practical data and investigated F-MWCNTs/EG-water nanofluids. They used the correlations to evaluate the PD and HTC. It is reported that a decrease in PD with rising shear rate and an increase with rising concentration and temperature. They concluded that for higher shear rate operating conditions F-MWCNTs/EG-water nanofluids is a proper choice. Contreras et al. [17] investigated the thermal and flow performance of EG/water based silver and graphene nanofluids in vehicle radiators. They reported augmentation of pumping power by 4.1% at high temperatures and mass flow rates. They concluded silver nanofluid improved the HT by 4.4% however the thermo-hydraulic performance worsened with graphene nanofluid. Abbas et al. [18] investigated the Fe_2O_3–TiO_2/water hybrid nanofluids application in aluminum tube vehicle heat exchangers. They performed an experimental study for a range of operating conditions 0.005, 0.007 and 0.009 vol%, inlet temperature from 48 to 56∘C and flow rate from 11 to 15 LPM. The inlet temperature reduced the HT by %8 and at higher concentrations due to unstable mixture the performance reduced significantly. Contreras et al. [19] investigated the radiators which are operating at high temperature using the MWCNT nanofluid experimentally for altering concentration, inlet temperature and they assessed the HT rate and overall HTC practically. The heat transfer performance improved with higher volume fraction and worsened with raising temperature at the inlet.

The vehicle heat exchangers usually designed using the welded and flattened tubular systems. Under identical operating conditions the novel double-U grooved and brazed tubes are compared with heavy duty vehicle heat exchangers designed with usual tubular systems. In current practical work, the effect of the flow rate of the coolant and the air velocity on thermal performance of four dissimilar truck radiators is researched. The HEs are evaluated in terms of HT rates, exit temperatures, total HTC and PDs. The practical outputs are associated with ε-NTU analysis and they show an agreement with an error less than 10% for all studied cases.

2. Experimental method

2.1. Experimental setup

Four different heavy truck radiators are studied practically for different working conditions and the consequence of altering parameters are discussed for HT rate, f and PD. The working fluid is a blend of 50:50 vol. DI water- EG. The radiators geometry details are given in Table 1. The experimental set up is shown in Fig. 1. Flattened and welded aluminum tube is used in R1 and R2. Double u-grooved and brazed aluminum tube is used in R3 and R4. Fin is used in all radiators with a constant geometrical parameters as $H_f = 0.1$ mm and $W_f = 7.8$ mm. The flattened pipes hydraulic diameter $D_h = 3.931$ mm, and the double-U grooved hydraulic diameter $D_h =$

2.531 mm. Aspect ratio of flattened pipe is 19.51 and 29.15 for U-grooved tubes.

The working conditions are summarized in Table 2. The measurements are performed after the steady state is reached. In Fig. 2, the whole specially equipped test chamber is shown. Water/EG and air side temperatures and pressures are collected with 50 Hz frequency.

2.2. Experimental validation

The hydro thermal characteristics and overall HT coefficient are assessed for altering working parameters for four vehicle radiators. The working conditions are given in Table 2.

The evaluated HT rates are compared with the measured data assessed with ε-NTU technique and an excellent compatibility is attained. The bulk temperatures are used to calculate the thermal specifications of the water/EG blend and the air. The bulk temperatures for water/EG and air ($T_{b,f}$, $T_{b,a}$) are evaluated using the in and out temperatures using the following equations:

$$T_{b,f} = \frac{(T_{f,i} + T_{f,o})}{2} \tag{1}$$

$$T_{b,a} = \frac{(T_{a,i} + T_{a,o})}{2} \tag{2}$$

The fluid and air side heat transfer rates:

$$\dot{Q}_f = \dot{m}_f \cdot C_f \cdot (T_{f,i} - T_{f,o}) \; \textit{for} \text{ water/EG,} \tag{3}$$

$$\dot{Q}_a = \dot{m}_a \cdot (h_{a,o} - h_{a,i}) \; \textit{for air} \tag{4}$$

here $\dot{m}$ is the mass flow rate, C is the specific heat, T is the temperature, h is enthalpy, the subscript f is for water/EG, a is for air, i is for inlet and o is for outlet.

The friction factor in the water/EG side reads

$$f = \frac{(2 \cdot \Delta P_f \cdot D_h)}{(L_{rad} \cdot N \cdot \rho_f \cdot u^2)} \tag{5}$$

The Re in the water/EG and air sides:

$$Re_f = \frac{(\rho_f \cdot u_f \cdot D_h)}{\mu_f} \tag{6}$$

$$Re_a = \frac{(\rho_a \cdot u_a \cdot W_a)}{\mu_a} \tag{7}$$

here W_a is the fin-width at the air side. The overall HTC found using the data is

$$U_{exp} = \frac{(\dot{Q}_{exp})}{LMTD \cdot F \cdot \pi \cdot D_h \cdot H_{rad} \cdot N} \tag{8}$$

$$LMTD = \frac{(T_{f,i} - T_{a,o}) - (T_{f,o} - T_{a,i})}{\ln\left(\frac{(T_{f,i} - T_{a,o})}{(T_{f,o} - T_{a,i})}\right)} \tag{9}$$

here $\dot{Q}_{exp}$ is the HT rate in the water/EG side and F is the correction factor of cross flow. The total heat capacities are reads;

$$C_f = \dot{m}_f \cdot C_{p,f} \tag{10}$$

$$C_a = \dot{m}_a \cdot C_{p,a} \tag{11}$$

Table 1
Radiators' geometrical factors.

Design parameters	R1	R2	R3	R4
Radiator size $H_{rad} \times L_{rad} \times W_{rad}$ [mm^3]	660 × 868 × 40	760 × 868 × 40	660 × 868 × 40	760 × 868 × 40
Pipe size $H_p \times W_p$ [mm^2]	40 × 2.05	40 × 2.05	39.35 × 1.35	39.35 × 1.35
Number of louvered fins N_f	81	81	87	87
Number of pipes	80	80	86	86

R=Radiator.

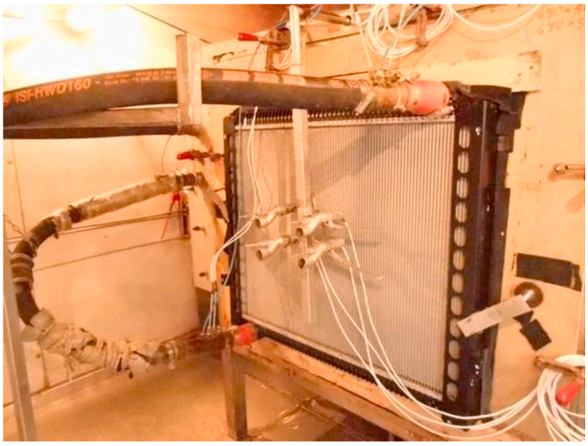

Fig. 1. Test section [20].

Table 2
Working conditions of the practical study.

Parameter	Range
Water/EG inlet temperature (Tc,i)	107 °C
Inlet air temperature (Ta,i)	40 °C
Inlet water/EG pressure (*Pc*,i)	100 kPa
Inlet air pressure (Pa,i)	150 kPa

Fig. 2. Photograph of the test chamber [20].

$$C_r = \frac{C_{min}}{C_{max}} \quad (12)$$

here C_r is the ratio of specific heat of the water/EG and air side.

$$Q_{max} = C_{min} \cdot \left(T_{f,i} - T_{a,i}\right) \quad (13)$$

$$Q_{estimate} = C_f \cdot \left(T_{f,i} - T_{f,o}\right) \quad (14)$$

here the effectiveness ε is defined as

$$\varepsilon = \frac{Q_{estimate}}{Q_{max}} \quad (15)$$

The NTU value then defined:

$$\mathrm{NTU} = \frac{1}{(C_r - 1)} \cdot \ln\left(\frac{\varepsilon - 1}{C_r \cdot \varepsilon - 1}\right) \tag{16}$$

$$U_{NTU} = \frac{(C_{min} \cdot NTU)}{\pi \cdot D_h \cdot H_{rad} \cdot N} \tag{17}$$

here NTU is the number of transfer units and U_{NTU} is the overall HTC.

The practical overall HTC is found using

$$U_{exp} = \frac{(\dot{Q}_{exp})}{LMTD \cdot F \cdot A}. \tag{19}$$

$$A = \pi \cdot D_h \cdot L_{rad} \cdot N. \tag{20}$$

3. Results and discussion

A cooling system of a vehicle is a set of components and working fluids to retain the engine's temperature at best possible values. This system composed of pump, coolant and thermostat and used in order to prevent the engine from break down due to overheating and complete the thermodynamic cycle. The cooling circuit is designed to maintain the engine temperature constant within certain limits. The radiator is a HE where the coolant is circulated and cooled down within the pipes and sent back to engine to absorb waste heat. During this process, the thermal capacity of the coolant, the design of the radiator, the exit temperature of the coolant, f and the PD plays essential role. In this study newly designed double-U grooved and brazed pipes are proposed for heavy duty vehicle radiators. The comparison with flattened and welded pipe is performed in terms of overall HT coefficient, HT rate, exit temperature and PD under changing operating conditions. Due to page limitation, only some of the important results and data could be given in this work.

The validation and accuracy of the experimental study is performed with a comparison between experimentally evaluated HT rates and analytical calculations. Additionally the experimental overall HT coefficient and the overall HT coefficient evaluated using the effectiveness-NTU method is compared for four dissimilar radiators designs. It is seen that in all design cases the mass flow rate increase enhanced the HT rate as well as the overall HT coefficient. The comparison is performed using ±10% error margin lines. In Fig. 3, the comparison for HT rate is shown for mass flow rate 3 kg/s for R1 and R4, for demonstration purposes. R1 both HT rates and overall HT coefficients are remained within the error margin. The error for R1 less than 5% and for the R4 the error is lower than 10%, see Fig. 3a and b shows the results for R1 and R4. The uncertainties inherited from the measurements causes the difference between the two results which should be the same under idealized case. Because of relatively low error margins, the experimental set up is acceptable and the insulation is satisfactory. Experimental overall HT coefficient is evaluated using equation (15); experimental overall HT coefficient is evaluated using equation (10). It is observed that for all design cases the findings are within the ±10% deviation bands. In Fig. 3c and d, only two radiator results are shown for mass flow rate 3 m/s for demonstration purposes and they show the results for R1 and R4 respectively.

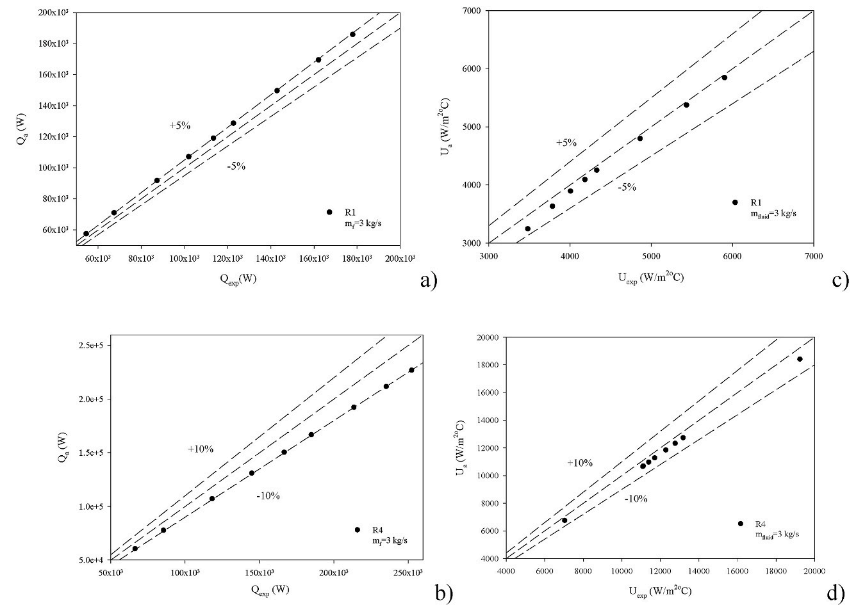

Fig. 3. Evaluation of practical and theoretical heat transfer rates and overall heat transfer coefficients determined by ε-NTU for rising air velocities at fixed coolant flow rate of 3 kg/s for Radiators 1 and 4.

For increasing water/EG Re the friction coefficient in the water/EG part and PD in the radiator is studied and the trend show similarities for altering air velocity. A characteristic tendency for f and PD is given in Fig. 4a and b, for $u_a = 12$ m/s. The friction coefficient reduces to some extent with increasing Re. The maximum f is found at the lowest water/EG Re for the R1. R3 demonstrated somewhat lesser friction coefficient compared to R4, which is because of the longer height of R4. The f reduced as the Re rose. The f is directly proportional to the water/EG viscosity at low Re. However, this observation is not valid at higher Re. For the higher Re, the f does not have a major dependence on water/EG viscosity, vortical structure of the operating fluid, and velocity has more important responsibility in raising the f. The consequence of viscosity is then less distinct [21]. Increased inertial forces reduce the friction force. The aerodynamic profile of the tubes used in the construction may lead lessened drag [22]. The complex flow characteristics and deceleration of the flow between the fins affects significantly the PD [23]. Augmented air flow rate does not alter the PD inside the radiator significantly. The highest PD is observed for R3 and R4 under same inertial effects.

A general observation for all radiator types is that the HT increased with rising water/EG mass flow rate (2.5 kg/s < $\dot{m}$ < 4.5 kg/s). The HT rate also increases with increasing air velocity (2 m/s < u_a < 12 m/s). For all operating conditions, R4 shows the highest HT rates. The HT rate of R2 and R3 shows close values at low air velocities. At low air velocities, such as $u_a = 2\ \text{m/s}$, the HT rates are ordered as $R1 < R2 < R3 < R4$. At moderate air velocities the order for R3 and R4 remains unchanged; however the performance of R1 and R2 performs identical. The behavior of HT rates of the radiators at low air velocities are observed at highest air velocity, $u_a = 10\ \text{m/s}$, and $u_a = 12\ \text{m/s}$. For increasing air velocities the enhancement in HT rates shows a steeper gradient with rising mass flow rates. A similar behavior is observed for rising Re numbers.

The impact of rising air velocity on HT rate is illustrated in Fig. 5. The sequence of radiator performance is depicted whereas the influence of rising air velocity is steeper at lower ones and becomes less steep at higher ones. Overall HTC is a function of the convective HTC, as a result, for higher Re causes larger HT rates. Tendency lines on Fig. 5 validate the essential physical mechanism of the convective HT.

The sole effect of rising mass flow rate of water/EG and air velocity on the water/EG outlet temperature is studied as illustrated in Fig. 6. In all cases, the water/EG inlet temperature is fixed to $T_{f,in} = 107$ °C. It should be noted that for all radiator categories at constant air velocity the rising water/EG mass flow rate augments the water/EG temperature at the exit. However the water/EG exit temperature decreases with increasing EG/water mass flow rate at constant air velocity. This is due to the EG/water residence time reduces with growing mass flow rate. For all air velocities and mass flow rates, the largest temperature drop is obtained in R4.

4. Conclusion

In this experimental study, four different heavy duty vehicle radiators are compared under different working conditions. The radiators are compared with each other regarding with hydrothermal performance under dissimilar working conditions. The R1 and R2 have conventional configuration, equipped with flattened and welded pipes with 81 louvered fins and the height of R2 is longer. The R3 and R4 equipped with newly designed tubular system with double-U grooved and brazed pipes with 87 louvered fins and the height of the R4 is longer. The common observations:

a The hydro thermal characteristics increased with increases radiator length
b For the tested four radiator categories, the HT rate is augmented with rising flow rate of water/EG and air velocity. R3 and R4 performed better because they are installed with double U grooved and brazed tubes.
c The friction factor faintly alters with water/EG flow rate and the air velocity. The maximum f is evaluated for R1. The friction factors are equal for R3 and R4.
d The PD rises with increasing inertial forces.
e The R4 exhibits the highest PD and R1 exhibits the lowest PD.
f The practically measured overall HTC and ε-NTU technique is compared for all radiator types, the error margin is found to be lower than 10%. R4 exhibited the finest fit among the radiators.
g The double-U grooved pipe Radiator is observed to perform better in terms of heat transfer rate but higher PD penalty.

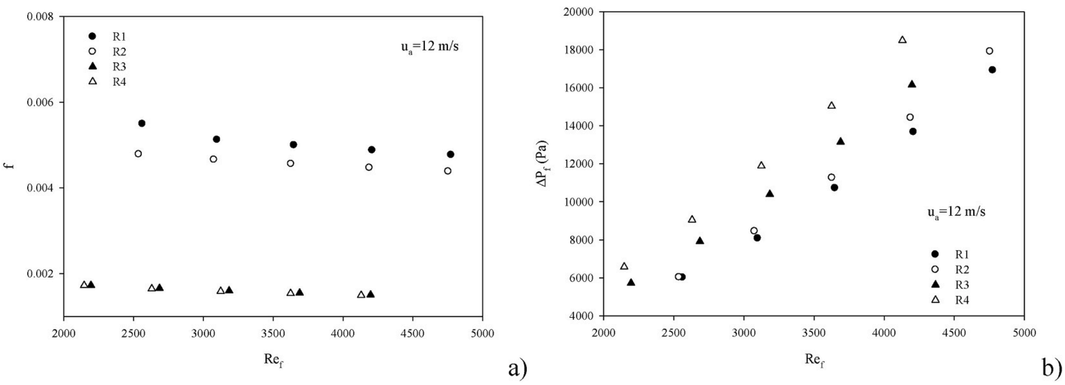

Fig. 4. Alteration of f (a) and PD (b) for rising Re of water/EG at u_a=12 m/s.

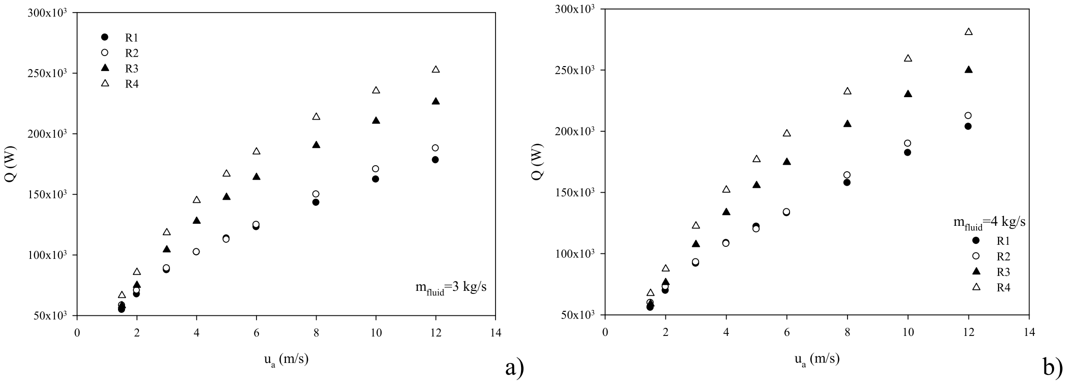

Fig. 5. Comparison of radiators for heat transfer rate alteration at increasing air velocities, and constant water/EG mass flow rate.

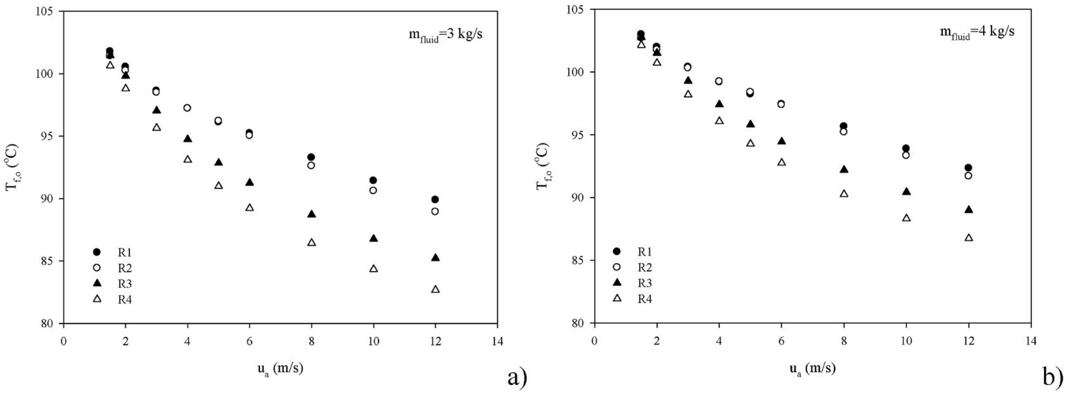

Fig. 6. Comparison of water/EG exit temperature at its constant mass flow rates of 3 kg/s (a), 4 kg/s (b) with increasing air velocities.

Authorship statement

Manuscript title: Experimental Comparison of Heat Transfer Characteristics of Enhanced Truck Radiators.

All persons who meet authorship criteria are listed as authors, and all authors certify that they have participated sufficiently in the work to take public responsibility for the content, including participation in the concept, design, analysis, writing, or revision of the manuscript. Furthermore, each author certifies that this material or similar material has not been and w ill not be submitted to or published in any other publication before its appearance in the Case Studies in Thermal Engineering.

1. Authorship contributions.

Please indicate the specific contributions made by each author (list the authors' initials followed by their surnames, e.g., Y.L. Cheung). The name of each author must appear at l east once in each of the three categories below.

1.1 Category 1.

Conception and design of study: A.S. Dalkilic,

acquisition of data: F Sonmez

analysis and/or interpretation of data: F. Sonmez, H. Mercan.

1.2 Category 2.

Drafting the manuscript: H Mercan, revising the manuscript critically for important intellectual content: A.S. Dalkilic, H. Mercan, S. Wongwises.

1.3 Category 3.

Approval of the version of the manuscript to be published (the names of all authors must be listed):

H. Mercan, F. Sonmez, A.S. Dalkilic, S. Wongwises.

2. Acknowledgements.

All persons who have made substantial contributions to the work reported in the manuscript (e.g., technical help, writing and editing assistance, general support), but who do not meet the criteria for authorship, are named in the Acknowledgements and have given us their written permission to be named. If we have not included an Acknowledgements, then that indicates that we have not received substantial contributions from non-authors.

Declaration of competing interest

The authors declare that they have no known competing financial interests or personal relationships that could have appeared to influence the work reported in this paper.

Acknowledgments

All four different heavy duty vehicle radiators were supplied by the Kale Oto Radyator A.S. The corroboration from the Kale Oto Radyator A.S. is gratefully acknowledged by the authors. The fourth author acknowledges the support provided by NSTDA under the Research Chair Grant, and the Thailand Science Research and Innovation (TSRI) under Fundamental Fund 2022.

Nomenclature

A	heat transfer area, m^2
C	specific heat, kJ/kgK
D_h	hydraulic diameter, m
EG	ethylene glycol
F	correction factor for cross flow
f	friction factor
H	height, m
HE	heat exchanger
HT	heat transfer
HTC	heat transfer coefficient, W/m^2K
L_{rad}	radiator length, m
LMTD	logarithmic average temperature difference, ^oC
$\dot{m}$	mass flow rate, kg/s
N	pipe number
PD	pressure drop, Pa
R	radiator
Re	Reynolds number
T	temperature, ^oC
u	velocity, m/s
$\dot{Q}_{exp}$	heat transfer rate obtained from the experiment, W
W	width, m
1,2,3,4	radiator numbers

Subscripts

a	air
exp	experimental
f	water/EG
i	inlet
o	exit
r	ratio
rad	radiator

References

[1] D.G. Charyulu, G. Singh, J.K. Sharma, Performance evaluation of a radiator in a diesel engine—a case study, Appl. Therm. Eng. 19 (6) (1999) 625–639.
[2] B. Rahmatinejad, M. Abbasgholipour, B. Mohammadi Alasti, Redesign of engine radiator based on number of optimal fans using a genetic algorithm, Karafan Q. Sci. J. 17 (4) (2021) 97–115.
[3] J.A. Akpobi, S.M.G. Akele, I. VI, E. Ao, A. Oj, Finite element analysis to predict temperature and velocity distribution in radiator tubes, Intern. J. Eng. Manag. Res. 9 (2019).
[4] K.A. Hamid, W.H. Azmi, R. Mamat, K.V. Sharma, Heat transfer performance of TiO2–SiO2 nanofluids in a tube with wire coil inserts, Appl. Therm. Eng. 152 (2019) 275–286.
[5] K. Bilen, M. Cetin, H. Gul, T. Balta, The investigation of groove geometry effect on heat transfer for internally grooved tubes, Appl. Therm. Eng. 29 (4) (2009) 753–761.
[6] P. Murugesan, K. Mayilsamy, S. Suresh, Turbulent heat transfer and pressure drop in tube fitted with square-cut twisted tape, Chin. J. Chem. Eng. 18 (4) (2010) 609–617.
[7] S. Eiamsa-Ard, P. Promvonge, Thermal characteristics of turbulent rib-grooved channel flows, Int. Commun. Heat Mass Tran. 36 (7) (2009) 705–711.
[8] S. Laohalertdecha, S. Wongwises, The effects of corrugation pitch on the condensation heat transfer coefficient and pressure drop of R-134a inside horizontal corrugated tube, Int. J. Heat Mass Tran. 53 (13–14) (2010) 2924–2931.
[9] W.T. Ji, A.M. Jacobi, Y.L. He, W.Q. Tao, Summary and evaluation on single-phase heat transfer enhancement techniques of liquid laminar and turbulent pipe flow, Int. J. Heat Mass Tran. 88 (2015) 735–754.

[10] H.A. Mohammed, A.N. Al-Shamani, J.M. Sheriff, Thermal and hydraulic characteristics of turbulent nanofluids flow in a rib–groove channel, Int. Commun. Heat Mass Tran. 39 (10) (2012) 1584–1594.

[11] R.K. Ajeel, W.I. Salim, K. Hasnan, Thermal and hydraulic characteristics of turbulent nanofluids flow in trapezoidal-corrugated channel: symmetry and zigzag shaped, Case Stud. Therm. Eng. 12 (2018) 620–635.

[12] R. Kocheril, J. Elias, Comparison of heat transfer rate with aluminium based nano Fluid and magnetised ferro fluid in internal combustion engine heat exchanger, J. Adv. Res. Fluid Mech. Thermal Sci. 67 (1) (2020) 170–177.

[13] V. Salamon, S. Thirumalini, Experimental investigation of heat transfer characteristics of automobile radiator using tio2-nanofluid coolant, in: IOP Conference Series: Materials Science and Engineering, vol. 225, IOP Publishing, 2017, August, 012101, 1.

[14] K. Goudarzi, H. Jamali, Heat transfer enhancement of Al2O3-EG nanofluid in a car radiator with wire coil inserts, Appl. Therm. Eng. 118 (2017) 510–517.

[15] Z. Said, M.E.H. Assad, A.A. Hachicha, E. Bellos, M.A. Abdelkareem, D.Z. Alazaizeh, B.A. Yousef, Enhancing the performance of automotive radiators using nanofluids, Renew. Sustain. Energy Rev. 112 (2019) 183–194.

[16] E. Shahsavani, M. Afrand, R. Kalbasi, Using experimental data to estimate the heat transfer and pressure drop of non-Newtonian nanofluid flow through a circular tube: applicable for use in heat exchangers, Appl. Therm. Eng. 129 (2018) 1573–1581.

[17] E.M.C. Contreras, G.A. Oliveira, E.P. Bandarra Filho, Experimental analysis of the thermohydraulic performance of graphene and silver nanofluids in automotive cooling systems, Int. J. Heat Mass Tran. 132 (2019) 375–387.

[18] F. Abbas, H.M. Ali, M. Shaban, M.M. Janjua, T.R. Shah, M.H. Doranehgard, F. Farukh, Towards convective heat transfer optimization in aluminum tube automotive radiators: potential assessment of novel Fe2O3-TiO2/water hybrid nanofluid, J. Taiwan Inst. Chem. Eng. 124 (2021) 424–436.

[19] E.M.C. Contreras, E.P. Bandarra Filho, Heat transfer performance of an automotive radiator with MWCNT nanofluid cooling in a high operating temperature range, Appl. Therm. Eng. 207 (2022), 118149.

[20] H.F. Sonmez, Ağır Ticari Araçlarda Radyatör Kapasitesinin Deneysel Olarak Tayini, Masters Thesis, YTU, Istanbul, 2019.

[21] P. Samira, Z.H. Saeed, S. Motahare, K. Mostafa, Pressure drop and thermal performance of CuO/ethylene glycol (60%)-water (40%) nanofluid in car radiator, Kor. J. Chem. Eng. 32 (4) (2015) 609–616.

[22] T.A. Tahseen, Rahman, M. Ishak, Experimental study on heat transfer and friction factor in laminar forced convection over flat tube in channel flow, Procedia Eng. 105 (2015) 46–55.

[23] M.E. Olson, Aerodynamic effects of front end design on automobile engine cooling systems, SAE Tech. Pap. Ser. 1 (2010) 883–892.